Cancer Research

Development of a T-cell Receptor Mimic Antibody against Wild-Type p53 for Cancer Immunotherapy

Demin Li[1], Carol Bentley[1], Amanda Anderson[1], Sarah Wiblin[1], Kirstie L.S. Cleary[2], Sofia Koustoulidou[3], Tasneem Hassanali[1], Jenna Yates[1], Jenny Greig[1], Marloes Olde Nordkamp[1], Iva Trenevska[1], Nicola Ternette[4], Benedikt M. Kessler[5], Bart Cornelissen[3], Mark S. Cragg[2], and Alison H. Banham[1]

Abstract

The tumor suppressor p53 is widely dysregulated in cancer and represents an attractive target for immunotherapy. Because of its intracellular localization, p53 is inaccessible to classical therapeutic monoclonal antibodies, an increasingly successful class of anticancer drugs. However, peptides derived from intracellular antigens are presented on the cell surface in the context of MHC I and can be bound by T-cell receptors (TCR). Here, we report the development of a novel antibody, T1-116C, that acts as a TCR mimic to recognize an HLA-A*0201–presented wild-type p53 T-cell epitope, $p53_{65–73}$(RMPEAAPPV). The antibody recognizes a wide range of cancers, does not bind normal peripheral blood mononuclear cells, and can activate immune effector functions to kill cancer cells *in vitro*. *In vivo*, the antibody targets $p53_{65–73}$ peptide–expressing breast cancer xenografts, significantly inhibiting tumor growth. This represents a promising new agent for future cancer immunotherapy. *Cancer Res; 77(10); 2699–711. ©2017 AACR.*

Introduction

Classical therapeutic antibodies commonly target cell surface or secreted antigens but are unable to access intracellular proteins. However, intracellular proteins are degraded by proteasome-dependent and -independent mechanisms, resulting in the generation of peptides for surface presentation by MHC class I (1). This presentation of peptides derived from intracellular proteins on the cell surface is part of the normal cellular process enabling the recognition of intracellular antigens by the immune system, in particular $CD8^+$ T cells whose T-cell receptors (TCR) bind the MHC I–presented peptides to enable killing of cells expressing foreign antigens. Antibodies mimicking this ability of T cells to recognize MHC I–presented peptides, so-called TCR mimic (TCRm) or TCR-like antibodies, have been generated against several intracellular antigens presented by common human leukocyte antigen (HLA) haplotypes such as HLA-A*0201 (HLA-A2) and have demonstrated potential therapeutic efficacies in various models (2–4).

One of the most extensively studied tumor-associated antigens is the tumor suppressor p53, whose widespread deregulation and involvement in malignant transformation make it an almost universal target for the immunotherapy of cancer (5). p53-derived peptides have been investigated as targets in various immunotherapy strategies including vaccines, recombinant TCRs, and TCRm antibodies (6–8). Missense mutations in *TP53* commonly lead to an accumulation of p53 protein in the cytosol, which leads to enhanced processing (of both wild-type and mutant peptides) by the antigen processing machinery (9). Evidence from studying the humoral immune responses in patients with cancer is that they recognize both wild-type and mutant p53 epitopes, without mutant p53-containing immunodominant epitopes (10). The diversity of *TP53* mutations, scarcity of mutant p53-derived T-cell epitopes (11, 12), and alternative mechanisms that regulate the wild-type p53 protein make immunotherapeutic strategies targeting wild-type p53 epitopes more broadly applicable and thus these have been actively pursued in a clinical setting (13–15).

Here, we report the production of a novel TCRm antibody targeting a wild-type p53-derived peptide and its potential application in tumor immunotherapy.

Materials and Methods

Cell culture

The following cell lines were purchased from ATCC in 2014: A2058, AU565, CALU6, COR-L23, G361, Hs-695T, MDA-MB-231, NCI-H1299, NCI-H1395, NCI-H1930, NCI-H1975, NCI-H2087, and PANC-1. Colo-205 was purchased from ATCC in 2015. The following cell lines were purchased from German Collection of Microorganisms and Cell Cultures (DSMZ): OCI-Ly1 (2004), OCI-Ly8 (2004), SW480 (2004), Granta-519 (prior to 2000), and KM-H2 (prior to 2000). MDA-MB-453, MDA-MB-468, T47D, and MCF-7 were obtained from Cancer Research

[1]Nuffield Division of Clinical Laboratory Sciences, Radcliffe Department of Medicine, University of Oxford, John Radcliffe Hospital, Headington, Oxford, United Kingdom. [2]Antibody & Vaccine Group, Cancer Sciences Unit, Faculty of Medicine, University of Southampton, Southampton General Hospital, Southampton, United Kingdom. [3]CRUK/MRC Oxford Institute for Radiation Oncology, Department of Oncology, University of Oxford, Oxford, United Kingdom. [4]The Jenner Institute, Nuffield Department of Medicine, University of Oxford, Oxford, United Kingdom. [5]Target Discovery Institute, Nuffield Department of Medicine, University of Oxford, Oxford, United Kingdom.

Note: Supplementary data for this article are available at Cancer Research Online (http://cancerres.aacrjournals.org/).

Corresponding Authors: Alison H. Banham, Nuffield Division of Clinical Laboratory Sciences, University of Oxford, Radcliffe Department of Medicine, John Radcliffe Hospital, Headington, Oxford, OX3 9DU, United Kingdom. Phone: 44-0-1865-220246; Fax: 44-0-1865-220980; E-mail: alison.banham@ndcls.ox.ac.uk; and Demin Li. Phone: 44-0-1865-220993; E-mail: demin.li@ndcls.ox.ac.uk

doi: 10.1158/0008-5472.CAN-16-3247

UK Claire Hall Laboratories (London, UK) in 2004. CCRF-CEM, HUT 78, KARPAS-299, and RPMI-8402 were from Georges Delsol (University of Toulouse, Toulouse, France) between 2000 and 2004. Daudi and Jurkat were obtained from the Sir William Dunn School of Pathology (University of Oxford, Oxford, UK) prior to 2000. OCI-Ly3 and SU-DHL-6 were from Dr. Eric Davis (NIH, Bethesda, MD) in 2000. MO1043 was obtained from Riccardo Dalla-Favera (Columbia University, New York, NY) in 2014; T2 and HL-60 from Alain Townsend (University of Oxford) prior to 2000; and 143B from Dr. Judy Bastin (University of Oxford) in 2015. MOLT-4 was obtained from Neckar Hospital prior to 2000. Colo-678 was from Walter Bodmer (University of Oxford) in 2013. Thiel was from Diehl (University of Cologne, Cologne, Germany). FL-18 was from Shirou Fukahara (Kyoto University, Kyoto, Japan) prior to 2000. SU-DHL-1 was from Dr. Steve Morris (St. Jude Children's Hospital) prior to 2000.

Hematologic cell lines were cultured in RPMI containing 10% FBS (Life Technologies, #10082147) and others in DMEM containing 10% serum, supplemented with penicillin/streptomycin (100 U/mL) and L-glutamine (2 mmol/L). The cells were cultured in 37°C incubators containing 5% CO_2. Experiments were performed using cells within maximum of 15 passages after thawing. The cell lines undergo periodic testing to ensure freedom from mycoplasma contamination using PlasmoTest Mycoplasma Detection kit (Invitrogen). MDA-MB-231 and Thiel were recently authenticated using STR profiling by LGC Standards, we experimentally performed the HLA-A2 and p53 expression profiling "in house".

Generation of HLA-A2 tetramers

A bacterial expression construct encoding the human HLA-A*0201 extracellular domain (amino acids 24–293) fused with a C-terminal BirA biotinylation sequence (LNDIFEAQKIEWH), and separate construct expressing mature human β2 microglobulin (β2m, amino acids 21-119), were each generated and transformed into competent *Escherichia coli* strain BL21(DE3). Protein expression was induced by addition of 0.5 mmol/L IPTG in low-salt LB medium (1% tryptone, 0.5% yeast extract, and 0.5% NaCl w/v), and insoluble inclusion bodies containing the recombinant proteins were purified using BugBuster (Merck, #70750-3), according to the manufacturer's instructions. Peptides were synthesized by the peptide synthesis facility in the Weatherall Institute of Molecular Medicine (University of Oxford).

HLA-A2 tetramers were generated as previously described (16, 17). Briefly, HLA-A*0201 (15 mg), β2m (12.5 mg), and peptide (5 mg) were added into 500 mL of refolding buffer (100 mmol/L Tris-HCl, pH 8.0, 400 mmol/L L-arginine, 2 mmol/L EDTA, 5 mmol/L reduced glutathione, 0.5 mmol/L oxidized glutathione, and 0.1 mmol/L phenylmethylsulfonylfluoride) and refolded for 48 hours. The refolding complex was concentrated and buffer exchanged to 10 mmol/L Tris-HCl, pH 8.0, and then biotinylated with BirA protein biotin ligase (Avidity LLC, #BirA500). Biotinylated protein was then separated using an Akta Purifier FPLC with a Sephadex 75 column, and HLA-A2/β2m/peptide monomers were isolated and subsequently stored at −80°C. Aliquots were thawed and tetramerized with Extravidin (Sigma-Aldrich, #E2511) on use.

Generation of anti-p53 TCRm monoclonal antibodies

All *in vivo* work was approved by local ethics review committee and governed by appropriate Home Office establishment, project and personal licenses. MF1 mice (6- to 8-week-old females) were immunized with the HLA-A*0201/p53 tetramers 4 times with 100 μg tetramer at 10-day intervals, and fusions were performed 2 days after the final immunization. A standard fusion protocol was followed (18) with NS0 murine myeloma cells as the fusion partner, and hybridomas were grown out under hypoxanthine, aminopterin, and thymidine (HAT) selection. Hybridoma supernatants were screened for the presence of secreted antibodies specifically, or preferentially, recognizing the immunizing tetramer rather than a control tetramer by ELISA. Positive hybridoma colonies were expanded and cloned by limiting dilution for further validation.

Production of purified antibodies

Production of purified TCRm antibodies from hybridoma supernatant was achieved by culturing hybridoma cells in serum-free medium to extinction or in CL350 bioreactors (Sigma-Aldrich, #Z688037), followed by protein A or protein G purification of immunoglobulin.

Endotoxin-free recombinant T1-116C antibody (mIgG1) production, and its isotype switching (mIgG2a or hIgG1), were outsourced to Absolute Antibody Ltd. after the antibody variable region cDNAs were cloned on the basis of a published method (19). Briefly, T1-116C heavy and light chains were cloned into pUV vectors and then transiently transfected into ABS293 cells. Culture supernatants were harvested and antibody-purified through Protein A affinity chromatography. Purified antibody was analyzed by SDS-PAGE, and endotoxin level was determined by LAL chromogenic endotoxin assay (Thermo Scientific, #88282).

T2 cell binding assay

TAP-deficient T2 cells cultured at logarithmic phase were pulsed with peptides at 100 mmol/L (or a range of lower concentrations for peptide titration experiments) for 12 to 16 hours in a flat-bottom 96-well tissue culture plate under standard cell culture conditions. Cells were then harvested and stained with TCRm antibodies and/or HLA-A2-specific mAb BB7.2 (Abcam, #ab74674), followed by alophycocyanin (APC)-conjugated goat anti-mouse secondary antibody (eBioscience, #17-4010-82). Samples were washed with FACS wash buffer (2% FBS in PBS + 0.1% sodium azide) and then fixed with 1% paraformaldehyde (in PBS) and acquired with a FACSCalibur (BD Biosciences).

Western blotting

Whole-cell lysates were prepared using Mammalian Protein Extraction Reagent (Thermo Scientific, 78503) containing a nuclease to degrade any nucleic acids and additional protease and phosphatase inhibitors. Protein concentrations were quantified using BCA assay (Thermo Scientific, 23227). Thirty micrograms of whole-cell lysates was resolved on 10% PAGE and transferred to Protran nitrocellulose membranes (GE Healthcare, 15269794). Membranes were blocked in 5% (w/v) low fat milk in PBS for 1 hour at room temperature and were then incubated with primary antibodies overnight at 4°C diluted in 5% (w/v) low fat milk in PBS: mouse anti-p53 (DO-1, Santa Cruz Biotechnology, sc-126, 1 μg/mL); mouse anti-p53 (DO-7, Santa Cruz Biotechnology, sc-47698, 1 μg/mL); mouse anti-p53 (Pab1801, Santa Cruz Biotechnology, sc-98, 1 μg/mL); and mouse anti-β-actin (Sigma, clone AC-15; 1:20,000). This was followed by washing of the membranes in PBS (3 washes) and PBS-Tween (0.1% v/v, one

wash) at room temperatures (5 minutes per wash) and then incubation in secondary antibody solution [goat anti-mouse IgG-HRP (Dako, P0447) diluted 1:5,000 in 5% (w/v) low fat milk in PBS] for 1 hour at room temperature. After washing as above, antibody binding was detected using ECL reagent (GE Healthcare, RPN2106) and visualized with a G:BOX ChemiXRQ imaging system (Syngene).

Mass spectrometry identifying HLA-I–associated peptides

Sample processing and data analysis were carried out as previously described (20). Briefly, 10^9 MDA-MB-231 and MCF-7 cells were lysed and cleared by centrifuging at 300 × *g* for 10 minutes at 4°C to remove nuclei, followed by 15,000 × *g* for 45 minutes at 4°C to pellet other insoluble material. HLA complexes were captured by rotating 1-mL W6/32–conjugated immunoresin (2.5 mg/mL) with the cleared lysates overnight at 4°C. Beads were re-packed in the column and washed by using subsequent runs of ice-cold 50 mmol/L Tris buffer (pH 8.0) containing first 150 mmol/L NaCl and 0.005% NP-40, then 150 mmol/L NaCl, followed by 400 mmol/L NaCl and lastly just 50 mmol/L Tris buffer. HLA-peptide complexes were eluted by using 5-mL ice-cold 10% acetic acid and dried. Samples were analyzed on an Ultimate 3000 HPLC system (Thermo Scientific) online coupled to a Q-Exactive Hybrid Quadrupole-Orbitra Mass Spectrometer (Thermo Scientific). Raw data were analyzed using Peaks 7.5 (Bioinformatics solutions) with a database containing all annotated human SwissProt entries.

Quantitation of antibody molecules bound per target cell

Cell lines or T2 cells pulsed with the RMPEAAPPV peptide at 0.5 to100 μmol/L concentrations or the Flu peptide at 100 μmol/L were stained with phycoerythrin (PE)-conjugated T1-116C mAb (mAb:PE = 1:1) or an isotype matched control antibody at 10 μg/mL for 30 minutes on ice. Cells were washed with FACS wash buffer and then fixed with 1% paraformaldehyde before being analyzed with a FACSCalibur (BD Biosciences). QuantiBRITE-PE beads (BD Biosciences, #340495) were acquired in parallel, and the correlation between geometric means (corrected to remove background binding to isotype control antibody) and PE molecules/beads of the 4 QuantiBRITE bead populations was established according to the manufacturer's instructions. The number of T1-116C-PE antibody molecules bound per cell was calculated on the basis of the correlation formula and subtraction of background from negative cells.

Complement-dependent cytotoxicity assay

A total of 1×10^5 cells were opsonized with antibody for 15 minutes at room temperature in a flat-bottom 96-well plate. Human serum was added to a final volume of 10% and incubated for 30 minutes at 37°C. Cells were transferred to a FACS tube where 10 μL propidium iodide (PI) solution (10 μg/mL in PBS) was added prior to data acquisition. Percentage cell death was defined as the percentage of PI^+ cells of the total cell population. Means from duplicate wells from each condition were calculated.

Antibody-dependent cellular phagocytosis assay

Mouse bone marrow–derived macrophages (BMDM) were differentiated from the bone marrow of wild-type BALB/c female mice and cultured for 7 to 10 days in the presence of 20% L929 conditioned media (containing macrophage colony-stimulating factor). A total of 5×10^4 BMDM per well were plated in a flat-bottom 96-well plate the day before the assay was performed as previously described (21). In brief, target cells were labeled with carboxyfluorescein succinimidyl ester (CFSE) at room temperature before being washed once in RPMI media. The CFSE-labeled cells were opsonized with antibody for 30 minutes at 4°C, washed once, and then 2.5×10^5 opsonized target cells were added to the BMDM and left to co-culture at 37°C for 1 hours. The BMDMs were labeled with anti-F4/80-APC (AbD Serotec, #MCA497APC) and the wells washed with PBS, before removal and analysis of the cells on FACSCalibur (BD Biosciences). Percentage of phagocytosis was defined as the percentage of $CFSE^+F4/80^+$ cells of the total $F4/80^+$ population. Means from triplicate wells from each condition were calculated.

Antibody-dependent cellular cytotoxicity assay

Human peripheral blood mononuclear cells (PBMC) isolated by density gradient centrifugation were sourced from the National Blood Service, and studies were conducted under ethical approval from the NRES Committee South Central – Oxford B (C06.216). Target cells were labeled with calcein AM (Life Technologies, #C1430) and suspended in RPMI. The labeled cells were opsonized with antibody for 30 minutes at 4°C before washing once in RPMI media. The target cells and PBMC effector cells were co-cultured at a 50:1 (effector:target) ratio for 4 hours at 37°C. The cells were pelleted by centrifugation (1,500 rpm for 5 minutes), the supernatant transferred to a white 96-well plate and read using a Varioskan Flash (Thermo Scientific) to record calcein release (excitation wavelength, 485 nm; emission wavelength, 530 nm). The percentage of maximum lysis was defined as calcein release compared with the response recorded when cells were treated with 4% Triton X-100 solution. Means from triplicate wells from each condition were calculated.

Antibody radiolabeling

T1-116C-mIgG2a and an isotype control antibody (Absolute Antibody Ltd.) were radiolabeled with ^{111}In as previously described (22). Briefly, 500 μg of T1-116C or isotype control antibody was dissolved in 0.1 mol/L sodium bicarbonate aqueous buffer (pH 8.2) before adding a 20-fold molar excess of 2-(4-isothiocyanatobenzyl)-diethylenetriaminepentaacetic acid (*p*-SCN-Bn-DTPA; Macrocyclics) and incubating for 1 hour at 37°C. The DTPA-conjugated antibody was subsequently purified using a Sephadex G50 gel filtration column and radiolabeled using ^{111}In-chloride (1MBq per 1μg of IgG). The protein was further purified by Sephadex G50 size exclusion chromatography. Radiochemical purity was determined by instant thin layer chromatography (iTLC) as more than 95%.

***In vivo* imaging and biodistribution**

Female BALB/c *nu/nu* mice (Charles Rivers Laboratories) were injected subcutaneously on their flanks with 1×10^6 MDA-MB-231 or MDA-MB-468 breast cancer cells. ^{111}In-labeled T1-116C or mIgG2a isotype control antibody (5 MBq, 5 μg) was administered intravenously when tumor sizes reached 120 mm^3 at day 20, and single-photon emission computed tomography (SPECT)/computed tomography (CT) imaging was performed at 24, 48, 72 hours after injection, using a Bioscan NanoSPECT/CT. Volume-of-interest analysis was performed on SPECT images using the Inveon Research Workplace Software Package (Siemens). After imaging at 72 hours postinjection, animals were sacrificed and

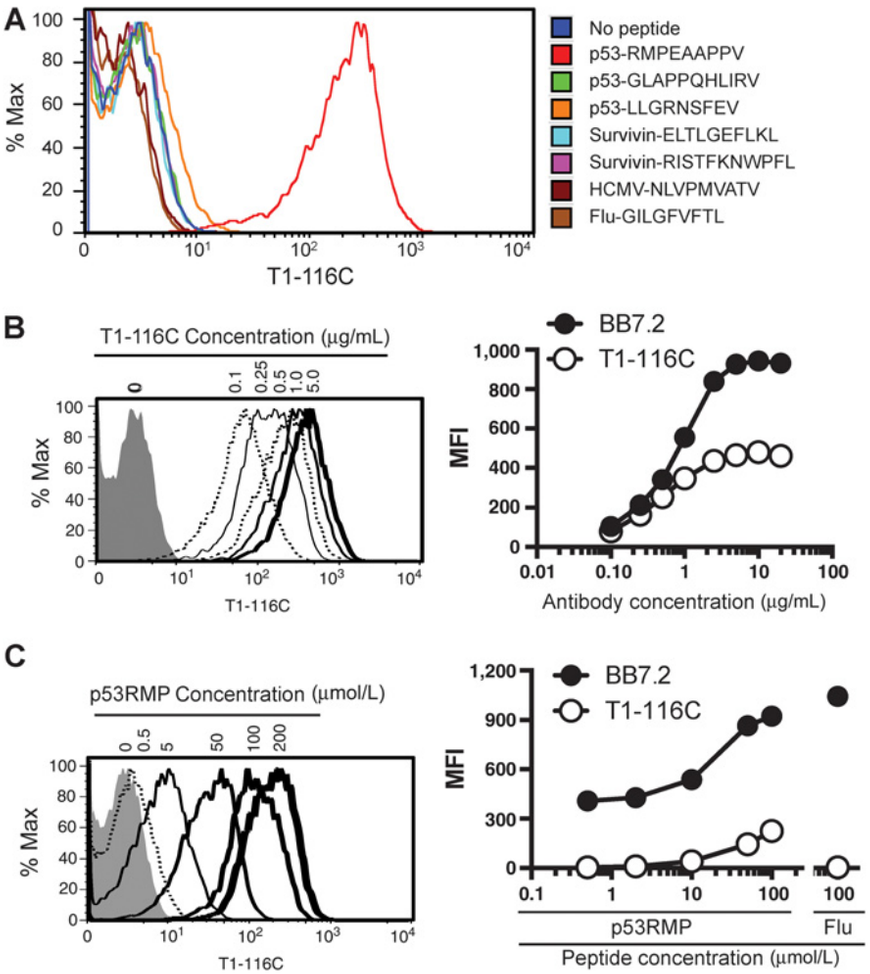

Figure 1.
Binding of the T1-116C TCRm antibody to p53RMP/HLA-A2 complexes on live cells detected by flow cytometry. **A,** T2 cells pulsed with p53RMP peptide at 100 μmol/L were stained with TCRm antibody supernatants and detected by an APC-conjugated anti-mouse secondary antibody. A panel of irrelevant peptides, including others derived from p53, was used as negative controls. **B,** T2 cells pulsed with p53RMP peptide at 100 μmol/L were stained with the purified T1-116 antibody at the indicated concentrations. HLA-A2–specific mAb BB7.2 was used in parallel to detect HLA-A2 expression. Mean fluorescence intensities (MFI) of the staining were plotted on the right panel (for clarity, the left panel does not contain all the tested concentrations). **C,** T2 cells pulsed with the p53RMP peptide at various concentrations were stained with the T1-116C antibody and the BB7.2 antibody against HLA-A2 at 10 μg/mL. Mean fluorescence intensities of the staining are plotted on the right. Flu peptide pulsing at 100 μmol/L was used as a negative control.

selected organs were removed, rinsed, blot dried, weighed, and the amount of ^{111}In in each tissue was measured using an automated gamma-counter. Uptake of ^{111}In was expressed as the percentage of the injected dose per gram of tissue (%ID/g).

Tumor *in vivo* growth experiments

MDA-MB-231 cells (1×10^7) in 100 μL Matrigel were injected subcutaneously into the flank of BALB/c *nu/nu* mice (Crl:NU-*Foxn1*^{nu}, 6–8 weeks, female, weight 15–22 g, Charles River Laboratories). Animals were randomly grouped, and antibodies or PBS was administered twice a week (10 mg/kg for Ab and 200 μL for PBS) by intraperitoneal injection. Tumor sizes were calculated as length × width × height × $\pi/6$. Geometric mean diameter (GMD) was calculated as $(L \times W \times H)^{1/3}$. The Student *t* test was used to evaluate the growth curves.

Results

Generation of p53/HLA-A2 murine monoclonal antibodies

A peptide derived from an N-terminal region of wild-type p53 that is rarely mutated was selected to enable targeting of the maximal number of potential patients, including those carrying the most common mutations leading to premature termination of p53 translation (R196X and R213X). This $p53_{65-73}$ peptide RMPEAAPPV (p53RMP) has also been proven to have endogenous presentation (23, 24) and has been tested in clinical trials of p53 vaccines without patients experiencing any adverse side effects (7). HLA-A2/p53RMP tetramers were produced and shown to be able to display the p53RMP peptide to T cells (Supplementary Fig. S1). These tetramers were used as the immunogen to generate TCRm mAbs recognizing p53RMP presented by HLA-A2 using classical hybridoma technology. Hybridoma supernatants were screened for reactivity against the immunizing p53RMP tetramer, and for specificity by their lack of binding to a tetramer comprising HLA-A2 with a non-related peptide derived from influenza A virus M1 protein (Flu), by ELISA. Unsurprisingly, the majority of the antibodies failed to demonstrate specificity for the p53RMP-containing tetramer and thus recognized the MHC portion of the complex (a representative example is illustrated in Supplementary Fig. S2).

The T1-116C hybridoma stably secreted antibodies recognizing the immunizing p53 tetramer but not the control tetramer by ELISA (Supplementary Fig. S2). Antibody-binding specificity toward the p53RMP peptide was further validated on the surface of human T2 lymphoblast cells. T2 cells are deficient in the transporter associated with antigen processing (TAP), and pulsing them with an HLA-A2–binding peptide

stabilizes the HLA-A2/peptide complex on the cell surface. T1-116C antibodies stained the cell surface of T2 cells pulsed with the target p53RMP peptide but not T2 cells pulsed with the Flu peptide, survivin, and HCMV peptides or non-target peptides derived from p53 (Fig. 1A).

The T1-116C antibody was protein A purified from the hybridoma supernatants and was further tested for a dose response in its binding to the p53RMP/HLA-A2 complex on the cell surface. T2 cells pulsed with the p53RMP peptide showed increased T1-116C binding when the antibody concentration increased; this was saturated at 5 μg/mL (Fig. 1B). Likewise, increasing peptide concentrations in the T2 cell assay also enabled increased T1-116C binding (Fig. 1C). On both the occasions, T1-116C binding was proportionally lower than that of the BB7.2 antibody, which detects HLA-A2 expression on the cell surface independently of the peptide being presented.

T1-116C binding is predominantly restricted to cancer cell lines with HLA-A2 and p53 expression

Having validated the specificity of T1-116C binding, we investigated whether the mAb could recognize the naturally processed p53RMP peptide presented on the surface of cancer cells. A panel of 39 cancer cell lines derived from various tissues was tested for T1-116C mAb binding and representative staining is shown in Fig. 2A. As summarized in Table 1, the T1-116C antibody was able to label cell lines derived from a variety of different cancer subtypes including lung cancer, osteosarcoma, colon cancer, breast cancer, melanoma, pancreatic cancer, and hematologic malignancies including chronic lymphocytic leukemia, follicular lymphoma, mantle cell lymphoma, and diffuse large B-cell lymphoma. The T1-116C antibody immunolabeling was almost exclusively restricted to HLA-A2$^+$ and p53$^+$ cancer cell lines, staining 68.2% (15 of 22) of the HLA-A2$^+$ cell lines (21 of which had confirmed p53 protein expression) but only one of the 17

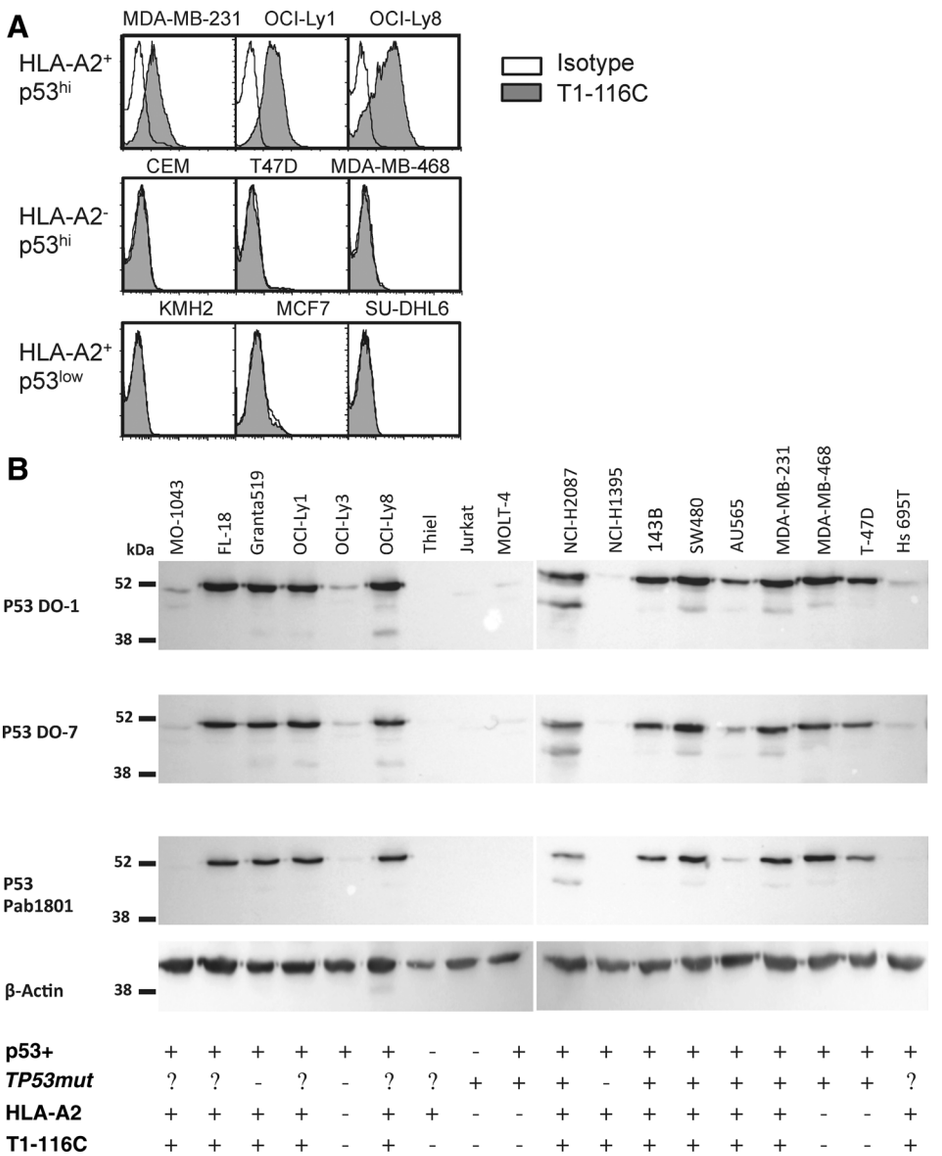

Figure 2.
T1-116C cell surface binding of cancer cells is typically HLA-A2 and p53-restricted. **A,** Cultured cancer cell lines were stained with the T1-116C antibody for FACS analysis. The cell lines recognized by T1-116C are commonly positive for both HLA-A2 and p53. T1-116C does not stain the majority of cell lines that are HLA-A2–negative, regardless of their p53 expression status. **B,** p53 protein expression in cancer cells detected by p53 mAbs DO-1, DO-7, and Pab1801. The status of p53 expression and mutation, as well as HLA-A2 expression and T1-116C staining, is summarized at the bottom of the panel. ?, *TP53* mutation status is unknown.

Table 1. Tumor cell expression of HLA-A2, p53, and their T1-116C binding

Cell line	Tumor	HLA-A2	*TP53* status	p53 protein	T1-116C
NCI-H2087	Lung	+	V157F	++	+
NCI-H1395	Lung	+	WT	+/−	+++
CALU6	Lung	−	R196stop	−	−
COR-L23	Lung	−	WT	−	−
NCI-H1299	Lung	−	WT/NULL	−	−
NCI-H1975	Lung	−	R273H	+++	−
NCI-H1930	Lung	+	G245R	++	−
A2058	Melanoma	−	V274F	+/−	−
G361	Melanoma	−		+/−	−
Hs-695T	Melanoma	+		+/−	++
143B	Osteosarcoma	+	R156P	+++	+
SW480	Colon	+	P309S, R273H	+++	++
Colo-205	Colon	+	G266E, Y103_L111>L	++	+
Colo-678	Colon	+	WT	++	+
AU565	Breast	+	R175H	+	+
MDA-MB-231	Breast	+	R280K	+++	++
MDA-MB-453	Breast	+	WT/MUT	±	−
MDA-MB-468	Breast	−	R273H	+++	−
MCF-7	Breast	+	WT	±	−
T47D	Breast	−	L194F	++	−
PANC-1	Pancreas	+	V272A, R273H	++	+
MO1043	CLL	+		+/−	++
FL-18	FL	+		+++	+
Granta 519	MCL	+	WT	+++	+++
OCI-Ly1	DLBCL	+		+++	++
OCI-Ly8	DLBCL	+		+++	+++
SU-DHL-6	DLBCL	+		++	−
OCI-Ly3	DLBCL	−	WT	+/−	−
KM-H2	cHL	+	WT	+/−	−
THIEL	Myeloma	+		−	−
Daudi	BL	−	G266Q R213stop	+	−
CCRF-CEM	T-ALL	−	R175H, R248Q	+++	−
MOLT-4	T-ALL	−	R248Q, R306stop	+/−	−
Jurkat	T-ALL	−	R196stop, T256A, D259G, S260A	−	−
RPMI 8402	T-ALL	−	R273C	++	−
HUT 78	CTCL	−	R196stop	+	−
KARPAS-299	ALCL	−	R273C	++	−
SU-DHL-1	ALCL	+		++	−
HL-60	APL	−	NULL	−	+

NOTE: HLA-A2 expression was detected by BB7.2 mAb staining. *TP53* status is indicated with the original amino acid, codon position, and alteration. Data were retrieved from the IARC *TP53* database (http://p53.iarc.fr/CellLines.aspx). WT/NULL and WT/MUT indicate either null or mutated *TP53* reported as well as wild-type in IARC *TP53* database. p53 protein expression was detected by Western blotting, and T1-116C staining was tested by FACS.

Abbreviations: ALCL, ALK$^+$ anaplastic large cell lymphoma; APC, acute promyelocytic leukemia; BL, Burkitt lymphoma; cHL, classical Hodgkin lymphoma; CLL, chronic lymphocytic leukemia; CTCL, cutaneous T-cell lymphoma; DLBCL, diffuse large B-cell lymphoma; FL, follicular lymphoma; MCL, mantle cell lymphoma; T-ALL, T-cell acute lymphoblastic leukemia; WT, wild-type *TP53*,.

HLA-A2$^-$ cell lines (11 of which expressed detectable p53 protein; Fig. 2B; Supplementary Fig. S3). There was no T1-116C labeling of the HLA-A2$^+$ Thiel cell line in which p53 protein expression was undetectable by either Western blotting (Fig. 2B) or immunocytochemistry (data not shown). However, HL-60 cells lacked both HLA-A2 and p53 protein expression and were bound by the T1-116C antibody (Supplementary Fig. S3). The epitope bound by T1-116C on HL-60 cells is as yet unknown, but the binding does not seem to represent epitope-independent binding by the Fc receptors expressed on HL-60 cells, as control antibodies with the same isotype did not bind.

Neither the level of p53 protein nor transcript expression was an accurate indicator of the intensity of T1-116C staining (Fig. 2B and Table 1; Supplementary Fig. S4). This is consistent with reports of p53 turnover, rather than steady-state levels, determining the presentation of epitopes by MHC class I to cytotoxic T lymphocytes (CTL; ref. 25). Proteasome inhibition using the inhibitor bortezomib significantly increased the levels of detectable p53 protein after 24 hours in NCI-H1395 cells (Supplementary Fig. S5). This demonstrates that p53 is normally actively being turned over in these cells and is consistent with this leading to p53 peptide presentation and strong T1-116C staining despite low levels of the p53 protein. T1-116C was able to recognize cell lines with either wild-type p53 or a variety of different *TP53* mutations. Interestingly, 3 (MDA-MB-435, MCF-7, and KMH2) of the 6 HLA-A2$^+$/p53$^+$ cell lines that were not stained by T1-116C had been reported in the International Agency for Research on Cancer (IARC) database as having wild-type *TP53* and only expressed low levels of the protein.

To further confirm that the p53RMP peptide is endogenously presented on cancer cells bound by T1-116C, we used mass spectrometry (MS) to identify HLA class I molecule–associated

peptides from 2 breast cancer cell lines: MDA-MB-231, which is recognized by T-116C, and MCF-7, which is not. The cells were lysed and immunoprecipitated with a pan-HLA class I antibody W6/32. Peptides associated with HLA class I complexes were isolated by high-performance liquid chromatography (HPLC) and their identities analyzed by liquid chromatography-tandem mass spectrometry (LC-MS/MS). No p53-derived peptide was identified from MCF-7 cells, whereas 4 such peptides were detected from MDA-MB-231 cells: KLLPENNVL (24–32), RMPEAAPRV (65–73), GLAPPQHLIRV (187–197), and LLGRNSFEV (264–272; Fig. 3A and B). All 4 peptides have been reported previously and 2 of them, GLAPPQHLIRV (187-197) and LLGRNSFEV (264-272), have been targeted by various immunotherapies (13, 26). The T1-116C target peptide isolated from MDA-MB-231 had the sequence RMPEAAP**R**V instead of RMPEAAP**P**V, reflecting a germline polymorphism at codon 72 reported to be associated with altered apoptosis-inducing function and hence increased cancer susceptibility (27). The change of proline at codon 72 to an arginine did not affect the binding of T1-116C as demonstrated by flow cytometry of a T2 stabilization assay (Fig. 3C).

The expression of p53 in normal tissues has been linked to radiation sensitivity, with hematopoietic tissues being among the normal adult tissues exhibiting the highest levels of p53 protein (28, 29). Normal circulating PBMCs have also been demonstrated to express the p53 protein (30). Flow cytometric analysis was performed to investigate whether normal PMBCs presented sufficient copies of the wild-type p53RMP peptide to enable binding of the T1-116C antibody. Of the 14 PBMC preparations from HLA-A2$^+$ donors, 13 (92.9%) were negative for T1-116C staining (Supplementary Fig. S6a). The single positive donor (Buf21), who only exhibited weak staining, had an abnormally high expansion of granulocytes (Supplementary Fig. S6b), which may be indicative of some potential abnormality. A nonexhaustive list of potential health problems associated with such granulocytosis includes leukemia, bacterial infection, and autoimmune disorders. These data indicate that the T1-116C antibody discriminates between p53$^+$/HLA-A2$^+$ normal and tumor cells. This is consistent with reports from studies using T cells that indicated that malignant cells have increased p53 epitope presentation (25, 31, 32).

Quantification of T1-116C binding to cancer cell lines and demonstration of engagement with immune effector cells to enable cell killing *in vitro*

The number of available epitopes present on the cell surface for antibody binding is an important determinant of therapeutic antibody activity (33). A standard curve of PE-coupled calibration beads (QuantiBRITE PE beads) was used to estimate

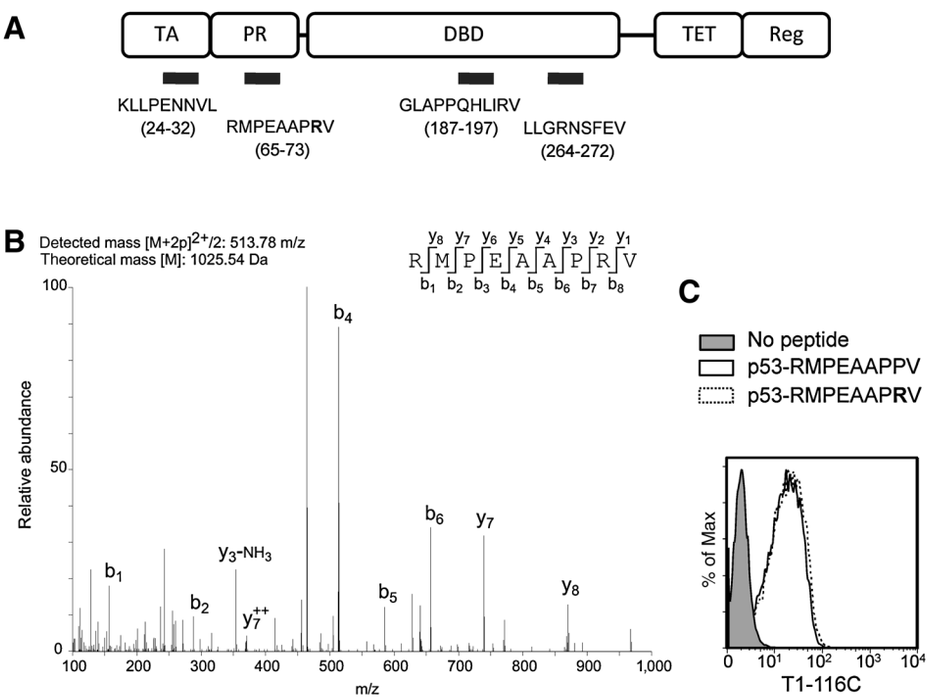

Figure 3.

MDA-MB-231 cells present p53RMP peptide that is detectable by T1-116C mAb. **A,** Diagram illustrating the p53-derived peptides identified by MS after MHC I immunoprecipitation from MDA-MB-231 cells. Black bars indicate the position of the peptides on p53 protein, and corresponding peptide sequences are labeled underneath the bars. DBD, DNA-binding domain; PR, proline-rich; Reg, regulatory region; TA, transactivation; TET, tetramerization domain. **B,** MS/MS spectrum of p53RMP detected from MDA-MB-231 breast cancer cells. The detected mass over charge ratio $[M+2p]^{2+}/2$ (p: protons) of the doubly charged peptide ion and the theoretical peptide mass [M] of the peptide are stated above the spectrum. All fragments that were detected are indicated in the peptide sequence. Most abundant fragment ions are assigned in the spectrum. Fragment ions are annotated as follows: b, N-terminal fragment ion; y, C-terminal fragment ion; y^{++}, doubly charged C-terminal peptide ion, $-NH_3$, ammonia loss. **C,** T1-116C binds both versions of p53RMP peptides in a T2 stabilization assay. The amino acid affected by the MDA-MB-231 p53 polymorphism is highlighted in bold.

the number of PE-conjugated T1-116C antibodies bound to the surface of peptide-pulsed T2 cells and cancer cell lines (Supplementary Table S1). T2 cells were pulsed with increasing concentrations of the p53RMP peptide. Approximately more than 150 bound T1-116C molecules per cell were detectable above background levels in this assay. This is comparable to $p53_{264-272}$/HLA-A2 TCR binding (200–300 binding sites per cell) detected using a soluble TCR with the same assay system (34). The tested cancer cell lines bound between 500 and 15,000 T1-116C-PE molecules per cell.

The original T1-116C mAb was a murine IgG1/κ isotype. For further functional studies, a human IgG1 chimeric antibody (hIgG1) and a mouse IgG2a (mIgG2a) antibody were generated by transferring the heavy and light chain variable regions of T1-116C into hIgG1 and mIgG2a backbones, respectively. The recombinantly produced antibodies retained the binding specificity of the original antibody purified from hybridoma supernatant (Fig. 4A).

Several TCRm antibodies against cancer targets have been shown to have *in vivo* activity against tumors by mediating immune effector mechanisms such as complement-dependent cytotoxicity (CDC), antibody-dependent phagocytosis (ADCP), and/or antibody-dependent cellular cytotoxicity (ADCC; refs, 4, 35, 36). The ability of a chimeric T1-116C antibody with a human IgG1 Fc domain to engage human immune effector cells was tested against B-cell lymphoma cell lines displaying high T1-116C binding, with rituximab (anti-CD20) used as a positive control (Fig. 4B). The T1-116C antibody was able to engage immune effector cells to kill both OCI-Ly1 and OCI-Ly8 B-cell lymphoma cell lines by ADCP, albeit less effectively than rituximab, with the highest dose (10 μg/mL) exhibiting the greatest effect. The T1-116C antibody did not convincingly demonstrate significant killing by ADCC. Intriguingly, the CDC killing mediated by T1-116C against OCI-Ly8 cells was higher than that achieved with rituximab at the two higher antibody concentrations.

T1-116C binds to and inhibits the growth of breast cancer xenografts *in vivo*

Antibody biodistribution *in vivo* gives a good indication of antibody uptake and clearance, including specific targeting to the tumor. For this purpose, T1-116C (mIgG2a) was conjugated to the metal ion chelator pSCN-BnDTPA, which allowed radiolabeling with ^{111}In chloride. The biodistribution of the radiolabeled antibody following intravenous administration (37) was compared with that of a nontargeting isotype control antibody in athymic mice bearing breast cancer xenografts that bind T1-116C *in vitro* (MDA-MB-231) or those that lack *in vitro* T1-116C binding (MDA-MB-468) using SPECT (Fig. 5A). Radiolabeled T1-116C and the isotype control followed a pattern of blood clearance, and tumor and tissue uptake that is consistent with other radiolabeled whole antibodies (37). Initially, the radiolabeled antibodies were observed in the blood, as indicated by the high signal in the heart, the carotid arteries, and the well-perfused liver. The amount of radiolabeled antibody in the blood then gradually decreased over time, whereas the uptake in the MDA-MB-231 tumor increased to more than 25% of the injected dose per gram (%ID/g) at 72 hours postinjection (Fig. 5B), thus increasing tumor-to-blood ratio, as indicated by tumor-to-heart uptake levels (Fig. 5C). MDA-MB-231 tumors, but not the MDA-MB-468 tumors, showed higher uptake of T1-116C ($P < 0.001$ at 48 hours postinjection)

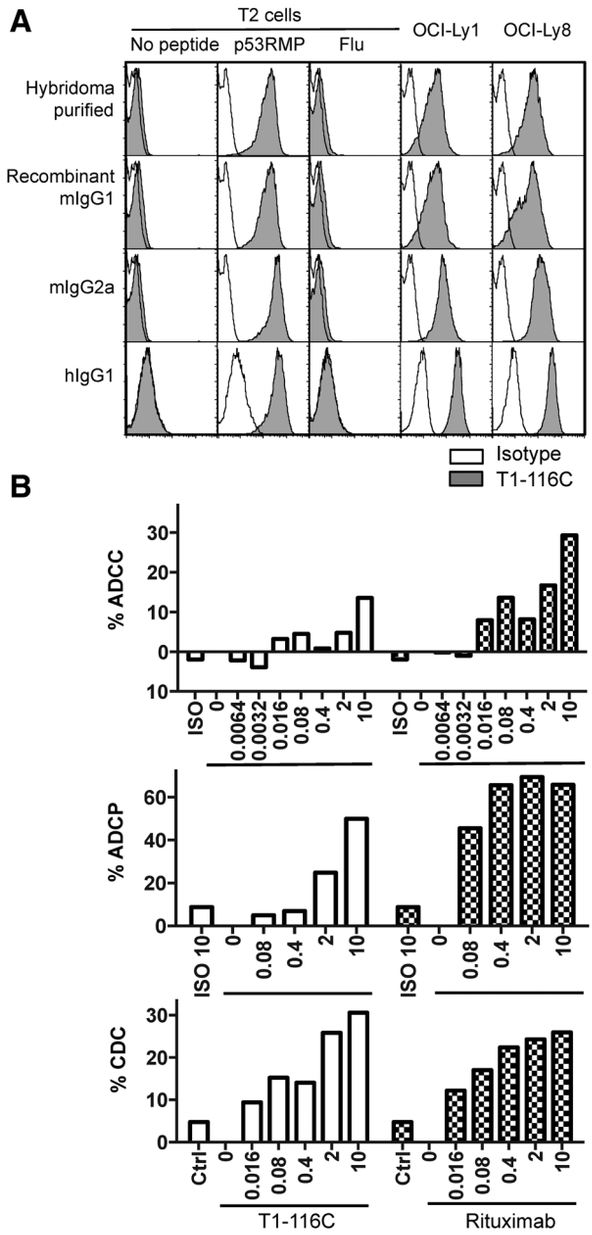

Figure 4.

The p53 TCRm T1-116C antibody can engage immune effector functions to achieve target cell killing. **A,** Validation of recombinantly expressed T1-116C antibodies. T2 cells pulsed with p53RMP or Flu peptide, along with OCI-Ly1 and OCI-Ly8 lymphoma cells, were stained with the original T1-116C (hybridoma purified) and recombinant T1-116C in mIgG1, mIgG2a, and hIgG1 isotypes. APC-conjugated anti-mouse or anti-human secondary antibodies were used to visualize the staining for flow cytometric analysis. **B,** Cytotoxicity of T1-116C against the B-cell lymphoma cell line OCI-Ly8 through immune effector functions. A human IgG1 chimeric form of T1-116C, at increasing concentrations (μg/mL), was used to induce human PBMC to exert ADCC (effector:target ratio = 50:1), mouse BMDM-mediated ADCP (effector:target ratio = 5:1), or human serum complement (10% v/v)-mediated CDC against OCI-Ly8 cells. The anti-CD20 mAb rituximab was used as a positive control. Herceptin was used as an isotype control antibody (Ctrl) at 10 μg/mL. One of three representing results are shown. Similar levels of ADCC and ADCP were observed against the B-cell lymphoma cell line OCI-Ly1 (data not shown).

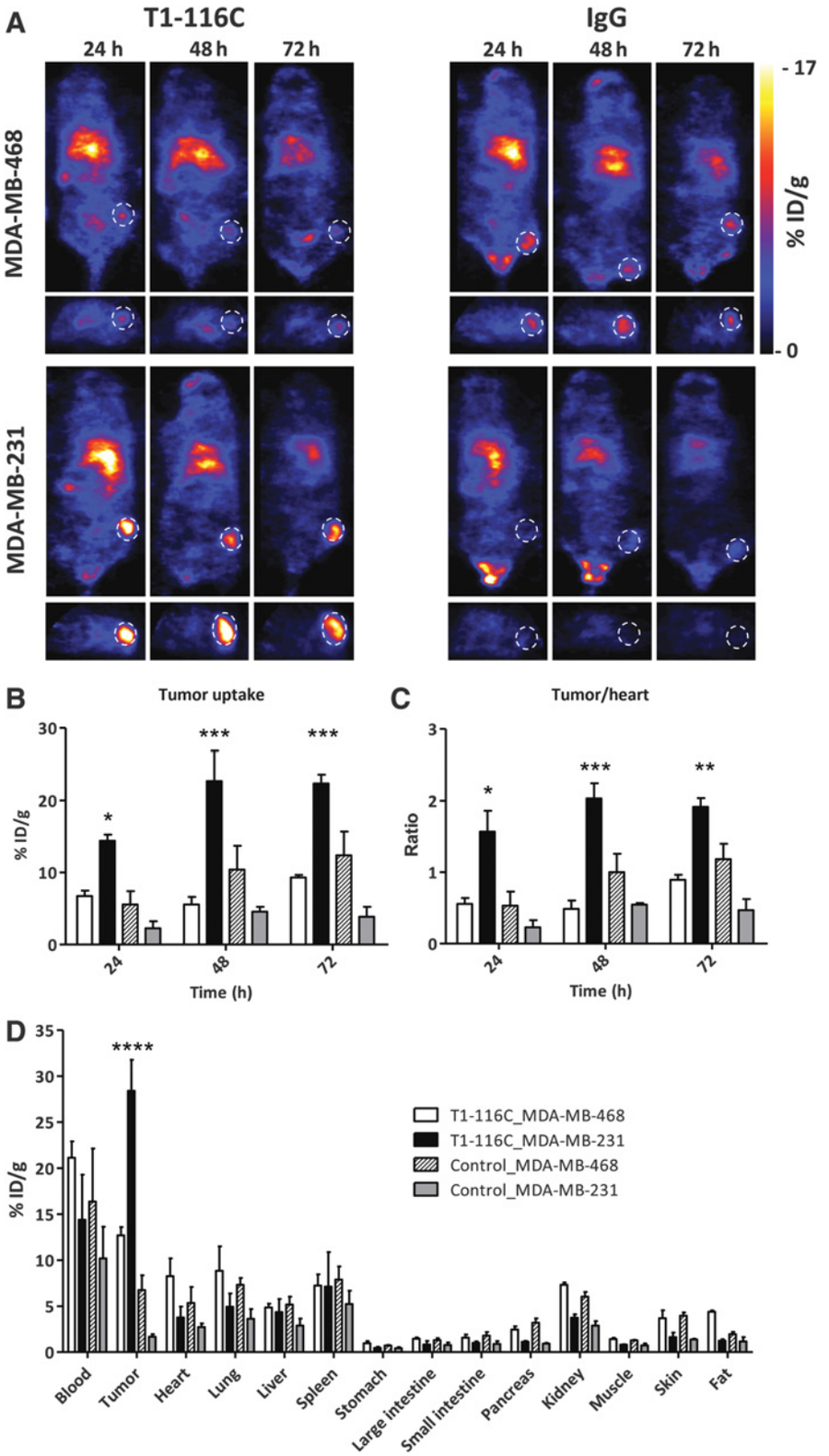

Figure 5.

T1-116C antibody biodistribution in athymic mice bearing MDA-MB-231 (**A**) or MDA-MB-468 (**B**) xenografts. Female BALB/c *nu/nu* mice were subcutaneously inoculated with 1×10^6 tumor cells that were allowed to grow until they reached 120 mm^3 at day 20. ^{111}In-labeled T1-116C ($n = 2$) or an isotype control ($n = 3$) was administered intravenously and SPECT/CT imaging performed at various times. Coronal (top) and transaxial (bottom) sections of SPECT images show high tumor uptake in athymic mice bearing MDA-MB-231 compared with MDA-MB-468 xenografts (**A**). Tumor uptake (**B**) and the ratio of antibody radio signals between tumor and heart (**C**) were calculated through volume-of-interest analysis on SPECT images. **D,** Biodistribution after dissection at 72 hours postinjection. *, $P < 0.05$; **, $P < 0.01$; ***, $P < 0.001$; ****, $P < 0.0001$ by ANOVA.

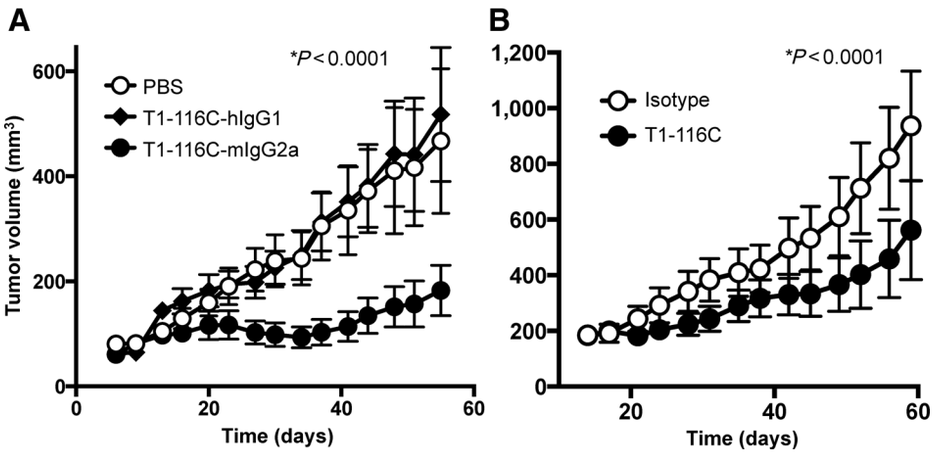

Figure 6.

The p53 TCRm T1-116C antibody inhibits tumor growth *in vivo*. **A,** T1-116C prevents engraftment of a triple receptor–negative breast cancer xenograft *in vivo*. A total of 1×10^7 human breast cancer MDA-MB-231 cells were injected subcutaneously into BALB/c *nu/nu* mice ($n = 10$ per group). T1-116C in two formats, a murine IgG2a isotype (mIgG2a) versus a human IgG1 isotype (hIgG1), or PBS carrier alone, was administered twice a week (10 mg/kg) starting from the time of tumor inoculation. **B,** T1-116C antibody delays MDA-MB-231 xenograft tumor growth. MDA-MB-231 cells were inoculated as described above, and the tumors were allowed to grow with treatment starting at day 14 when the average tumor sizes reached 150 mm^3. Mice were divided into groups having similar average tumor sizes and distributions ($n = 9$). T1-116C-mIgG2a and an isotype control antibody were injected twice a week (10 mg/kg) intraperitoneally until the end of the experiment. Tumor sizes were calculated as length × width × height × π/6.

compared with the isotype control antibody. Biodistribution after dissection (Fig. 5D) confirmed a significantly higher uptake of radiolabeled T1-116C in MDA-MB-231 tumor tissues compared with normal tissues ($P < 0.0001$), compared with MDA-MB-468 ($P < 0.0001$) and compared with the control antibody ($P < 0.0001$).

To investigate whether T1-116C antibody has any effect on *in vivo* tumor growth, recombinant T1-116C in either hIgG1 or mIgG2a formats was tested for their ability to prevent the engraftment of MDA-MB-231 tumors in BALB/c *nu/nu* mice (10 mg/kg, twice weekly). The T1-116C mIgG2a format antibody significantly inhibited tumor growth *in vivo* ($P < 0.0001$; Fig. 6A). The T1-116C hIgG1 format antibody did not significantly affect tumor growth. Although hIgG1 can bind all activating murine FcγRs, it has been reported to be less potent than mIgG2a antibodies in mouse models (38), which likely contributes to the differences observed.

The T1-116C mIgG2a antibody was further tested for its ability to prevent the growth of established MDA-MB-231 tumors in BALB/c *nu/nu* mice (Fig. 6B). Compared with an isotype matched control antibody (anti-fluorescein) or PBS carrier alone, the T1-116C antibody significantly reduced the growth rate of MDA-MB-231 tumors ($P < 0.0001$).

Discussion

p53 expression and epitope presentation can be affected by multiple mechanisms, including MDM2 overexpression, human papillomavirus (HPV) infection and $p14^{ARF}$ mutations (39). Generally, tumor cells are found to have higher copy numbers of wild-type p53 peptide-MHC class I complexes than normal cells (25, 31, 32). This is partly due to the increased turnover and thus processing of p53 in tumor cells (25) and partly due to the low levels of p53 in normal cells (40, 41). Consequently, CTLs recognizing wild-type p53 can discriminate between $p53^+$ tumor cells and normal tissues (42). Both CTLs and T helper (Th) cells directed against wild-type p53 have eradicated tumors *in vivo* without damage to normal tissues (43, 44). Importantly, high tumor levels of p53 are not a prerequisite for tumor killing by CTLs targeting wild-type p53 peptides, and such CTLs were able to kill tumors expressing low-level p53 protein. Interestingly, T-cell recognition of tumors without detectable p53 protein expression has been reported within the context of HPV infection, where enhanced p53 proteasomal degradation occurs (45). Thus, both wild-type and mutated p53 are among the top tumor antigens prioritized by a National Cancer Institute pilot project to accelerate translational research (5).

Vaccination studies utilizing a variety of wild-type p53 peptides (HLA-A2 restricted peptides comprising p53 amino acids 65–73, 149–157, 187–197, 217–255, and 264–272) and different vaccine delivery systems have been taken through to clinical trials (14, 15). While the vaccines were safe, able to induce anti-p53 immune responses, and some patients achieved stable disease, we are unaware of clinical responses with a significant reduction in tumor burden, which is consistent with most cancer vaccination studies, and is largely due to the immunosuppressive nature of the tumor microenvironment (14, 15). It is estimated that for CTL killing, the optimal number of binding sites on target cells is between 80 and 120, whereas higher concentrations (500–700) induce T-cell hyporesponsiveness (46, 47). Here, we detected 500 to 15,000 T1-116C molecules being bound to cancer cell lines and the potential contribution that this might make to T-cell unresponsiveness to the p53RMP epitope could be further investigated in vaccination studies. The high number of T1-116C molecules bound per cell is comparable to those bound by a TCRm antibody against the melanoma differentiation antigen tyrosinase (47). Fortunately, it is generally accepted that antibody-mediated function

correlates positively with the number of their binding sites on target cells (33).

TCRm antibodies circumvent the processes of immune cell priming and maturation, can directly recognize and bind peptide-presenting targets, and subsequently induce cytotoxicity through the components of the innate immune system such as natural killer cells, complement, and macrophages. As demonstrated in this study, TCRm T1-116C raised against the wild-type p53RMP peptide elicited all of these functions and impaired tumor growth *in vivo*, indicating promising therapeutic efficacy in a preclinical model of aggressive triple receptor–negative breast cancer, a malignancy that urgently needs improved therapeutic options.

Similar to TCRs, TCRm antibodies possess the ability to recognize multiple epitopes that have similar structures (4, 48). Such cross-reactivity potentially poses a risk for future clinical applications. We have so far observed that T1-116C binding requires both HLA-A2 and p53 expression in the cell lines we tested with the exception of the promyelocytic leukemia cell line, HL-60. This cell line is reported to express HLA-A*0101, HLA-B*5701, and HLA-C*0602 (49) and does not have detectable p53 expression. We have ruled out Fc receptor binding and cell line misidentification and have confirmed the lack of HLA-A2 expression on our laboratory stock of the cell line. Considering that no other HLA-A2$^-$ or p53$^-$ cell lines, nor normal PBMC samples, showed significant binding by this antibody, the ligand(s) bound on HL-60 is evidently not widely expressed. Further investigations are underway to characterize the amino acid dependency of T1-116C binding within the p53RMP peptide and to identify whether peptides derived from antigens other than p53 may also be recognized and thus provide an explanation for this potential off-target binding. However, in MDA-MB-231 cells, the p53RMP peptide was experimentally demonstrated to be co-immunoprecipitated with MHC class I by MS analysis of bound peptides, demonstrating its availability as a target epitope in the cell line used for the *in vivo* study. Interestingly, crystallization of the ESK1 TCRm antibody bound to its antigen Wilm's tumor 1 (WT1)/HLA-A2 recently demonstrated that the antibody bound its target differently to TCRs and indeed exhibited binding to multiple HLA-A*02 subtypes (50).

Murine antibodies cannot be repeatedly administered in man because of the development of immune responses against murine immunoglobulin epitopes. To enable T1-116C re-administration in patients, we humanized and de-immunized the antibody and showed that the recombinant hT1-116C antibody retains similar *in vitro* binding specificity to the original murine reagent (unpublished data). While immune effector functions engaged by the naked T1-116C might give the antibody sufficient potency against B-cell lymphomas, where antibodies against highly expressed B-cell differentiation antigens have proven effective, there may be additional arming strategies needed for efficacy in solid tumors. Dahan and Reiter (2) have recently comprehensively reviewed the mechanisms of action whereby TCRm antibodies can be used to target tumors. In general, their indications for therapeutic targeting of other agents are similar to those for TCRs, particularly following the successful engineering of high-affinity recombinant TCRs to overcome their naturally low affinity. These include the use of TCRm antibodies to deliver drugs or toxins, and their potential as a targeting moiety for tumor targeting viruses. Importantly, these approaches do not require a competent immune system and thus will be suitable for immunosuppressed patients lacking both immune effectors and T cells. TCRm antibodies also have the potential to be used as the targeting agent on chimeric antigen receptor (CAR)-engineered T cells, without any potential for recombining with endogenous TCRs. Future studies of multiple tumor models and normal tissue cross-reactivity profiling are required to evidence sufficient efficacy and specificity, but we believe this p53RMP TCRm antibody represents a promising new agent for future cancer immunotherapy.

Disclosure of Potential Conflicts of Interest

The authors are inventors (A.H. Banham, D. Li) and contributors (C. Bentley, A. Anderson, S. Wiblin, K.L.S. Cleary, S. Koustoulidou, T. Hassanali, J. Yates, J. Greig, B. Cornelissen, M.S. Cragg) on a patent application entitled 'T-cell receptor mimic (TCRm) antibodies.' B. Cornelissen has ownership interest in anti-p53/HLA-A*0201 T-cell receptor mimic antibody. M.S. Cragg is a consultant at Bioinvent International. No potential conflicts of interest were disclosed by the other authors.

Disclaimer

The views expressed are those of the author(s) and not necessarily those of the NHS, the NIHR or the Department of Health.

Authors' Contributions

Conception and design: D. Li, A.H. Banham

Development of methodology: D. Li, B.M. Kessler, B. Cornelissen, M.S. Cragg

Acquisition of data (provided animals, acquired and managed patients, provided facilities, etc.): D. Li, C. Bentley, A. Anderson, S. Wiblin, K.L.S. Cleary, S. Koustoulidou, J. Greig, M. Olde Nordkamp, I. Trenevska, N. Ternette, B.M. Kessler, B. Cornelissen

Analysis and interpretation of data (e.g., statistical analysis, biostatistics, computational analysis): D. Li, A. Anderson, J. Greig, M. Olde Nordkamp, N. Ternette, B.M. Kessler, B. Cornelissen, M.S. Cragg, A.H. Banham

Writing, review, and/or revision of the manuscript: D. Li, A. Anderson, I. Trenevska, N. Ternette, B.M. Kessler, B. Cornelissen, M.S. Cragg, A.H. Banham

Administrative, technical, or material support (i.e., reporting or organizing data, constructing databases): D. Li, S. Wiblin, T. Hassanali, J. Yates

Study supervision: D. Li, A.H. Banham

Acknowledgments

We would like to thank Professor Adrian Harris and Dr. Massimo Masiero for helpful discussions and Jose Orta for technical support.

Grant Support

This work was supported by Cancer Research UK (CRUK) program grant A10702 to A.H. Banham. B. Cornelissen and S. Koustoulidou were supported through the CRUK/Medical Research Council (MRC) Oxford Institute for Radiation Oncology. An MRC PhD studentship was given to S. Koustoulidou. Funding was provided through a studentship from the Biotechnology and Biological Sciences Research Council (BBSRC) to K.L.S. Cleary and Program Grants from Bloodwise (12050) and CRUK (A20537) to M.S. Cragg. M. Olde Nordkamp is supported by a project grant from Breast Cancer Now to D. Li. I. Trenevska is supported by a University of Oxford Medical Sciences Graduate School Studentship. The National Institute for Health Research (NIHR) Oxford Biomedical Research Centre program.

The costs of publication of this article were defrayed in part by the payment of page charges. This article must therefore be hereby marked *advertisement* in accordance with 18 U.S.C. Section 1734 solely to indicate this fact.

Received November 29, 2016; revised January 17, 2017; accepted March 9, 2017; published OnlineFirst March 31, 2017.

References

1. Rock KL, York IA, Goldberg AL. Post-proteasomal antigen processing for major histocompatibility complex class I presentation. Nat Immunol 2004;5:670–7.
2. Dahan R, Reiter Y. T-cell-receptor-like antibodies - generation, function and applications. Expert Rev Mol Med 2012;14:e6.
3. Weidanz JA, Hawkins O, Verma B, Hildebrand WH. TCR-like biomolecules target peptide/MHC Class I complexes on the surface of infected and cancerous cells. Int Rev Immunol 2011;30: 328–40.
4. Dao T, Yan S, Veomett N, Pankov D, Zhou L, Korontsvit T, et al. Targeting the intracellular WT1 oncogene product with a therapeutic human antibody. Sci Transl Med 2013;5:176ra33.
5. Cheever MA, Allison JP, Ferris AS, Finn OJ, Hastings BM, Hecht TT, et al. The prioritization of cancer antigens: a national cancer institute pilot project for the acceleration of translational research. Clin Cancer Res 2009;15:5323–37.
6. Fishman MN, Thompson JA, Pennock GK, Gonzalez R, Diez LM, Daud AI, et al. Phase I trial of ALT-801, an interleukin-2/T-cell receptor fusion protein targeting p53 (aa264–272)/HLA-A*0201 complex, in patients with advanced malignancies. Clin Cancer Res 2011;17:7765–75.
7. Svane IM, Pedersen AE, Johnsen HE, Nielsen D, Kamby C, Gaarsdal E, et al. Vaccination with p53-peptide-pulsed dendritic cells, of patients with advanced breast cancer: report from a phase I study. Cancer Immunol Immunother 2004;53:633–41.
8. Weidanz JA, Wittman, Vaughan VP, inventors. Antibodies as T cell receptor mimics, methods of production and use thereof 2005. Europe patent EP1773383 B1. 2012 Sep 12.
9. De Leo AB. p53-based immunotherapy of cancer. Approaches to reversing unresponsiveness to T lymphocytes and preventing tumor escape. Adv Otorhinolaryngol 2005;62:134–50.
10. Labrecque S, Naor N, Thomson D, Matlashewski G. Analysis of the anti-p53 antibody response in cancer patients. Cancer Res 1993;53: 3468–71.
11. Noguchi Y, Chen YT, Old LJ. A mouse mutant p53 product recognized by CD4+ and CD8+ T cells. Proc Natl Acad Sci U S A 1994;91:3171–5.
12. Yanuck M, Carbone DP, Pendleton CD, Tsukui T, Winter SF, Minna JD, et al. A mutant p53 tumor suppressor protein is a target for peptide-induced CD8+ cytotoxic T-cells. Cancer Res 1993;53:3257–61.
13. Theobald M, Offringa R. Anti-p53-directed immunotherapy of malignant disease. Expert Rev Mol Med 2003;5:1–13.
14. DeLeo AB, Whiteside TL. Development of multi-epitope vaccines targeting wild-type sequence p53 peptides. Expert Rev Vaccines 2008; 7:1031–40.
15. Vermeij R, Leffers N, van der Burg SH, Melief CJ, Daemen T, Nijman HW. Immunological and clinical effects of vaccines targeting p53-overexpressing malignancies. J Biomed Biotechnol 2011;2011:702146.
16. Ogg GS, McMichael AJ. HLA-peptide tetrameric complexes. Curr Opin Immunol 1998;10:393–6.
17. Altman JD, Moss PA, Goulder PJ, Barouch DH, McHeyzer-Williams MG, Bell JI, et al. Phenotypic analysis of antigen-specific T lymphocytes. Science 1996;274:94–6.
18. Kohler G, Milstein C. Continuous cultures of fused cells secreting antibody of predefined specificity. Nature 1975;256:495–7.
19. Brocks B, Garin-Chesa P, Behrle E, Park JE, Rettig WJ, Pfizenmaier K, et al. Species-crossreactive scFv against the tumor stroma marker "fibroblast activation protein" selected by phage display from an immunized FAP-/- knock-out mouse. Mol Med 2001;7:461–9.
20. Ternette N, Yang H, Partridge T, Llano A, Cedeno S, Fischer R, et al. Defining the HLA class I-associated viral antigen repertoire from HIV-1-infected human cells. Eur J Immunol 2016;46:60–9.
21. Tipton TR, Roghanian A, Oldham RJ, Carter MJ, Cox KL, Mockridge CI, et al. Antigenic modulation limits the effector cell mechanisms employed by type I anti-CD20 monoclonal antibodies. Blood 2015; 125:1901–9.
22. Cornelissen B, Kersemans V, Darbar S, Thompson J, Shah K, Sleeth K, et al. Imaging DNA damage *in vivo* using gammaH2AX-targeted immunoconjugates. Cancer Res 2011;71:4539–49.
23. Barfoed AM, Petersen TR, Kirkin AF, Thor Straten P, Claesson MH, Zeuthen J. Cytotoxic T-lymphocyte clones, established by stimulation with the HLA-A2 binding p5365–73 wild type peptide loaded on dendritic cells In vitro, specifically recognize and lyse HLA-A2 tumour cells overexpressing the p53 protein. Scand J Immunol 2000;51:128–33.
24. Würtzen PA, Pedersen LO, Poulsen HS, Claesson MH. Specific killing of P53 mutated tumor cell lines by a cross-reactive human HLA-A2-restricted P53-specific CTL line. Int J Cancer 2001;93:855–61.
25. Vierboom MP, Zwaveling S, Bos GMJ, Ooms M, Krietemeijer GM, Melief CJ, et al. High steady-state levels of p53 are not a prerequisite for tumor eradication by wild-type p53-specific cytotoxic T lymphocytes. Cancer Res 2000;60:5508–13.
26. Nijman HW, Van der Burg SH, Vierboom MP, Houbiers JG, Kast WM, Melief CJ. p53, a potential target for tumor-directed T cells. Immunol Lett 1994;40:171–8.
27. Soussi T, Wiman KG. Shaping genetic alterations in human cancer: the p53 mutation paradigm. Cancer Cell 2007;12:303–12.
28. MacCallum DE, Hupp TR, Midgley CA, Stuart D, Campbell SJ, Harper A, et al. The p53 response to ionising radiation in adult and developing murine tissues. Oncogene 1996;13:2575–87.
29. Dainiak N. Hematologic consequences of exposure to ionizing radiation. Exp Hematol 2002;30:513–28.
30. Maas K, Westfall M, Pietenpol J, Olsen NJ, Aune T. Reduced p53 in peripheral blood mononuclear cells from patients with rheumatoid arthritis is associated with loss of radiation-induced apoptosis. Arthritis Rheum 2005;52:1047–57.
31. Theobald M, Ruppert T, Kuckelkorn U, Hernandez J, Haussler A, Ferreira EA, et al. The sequence alteration associated with a mutational hotspot in p53 protects cells from lysis by cytotoxic T lymphocytes specific for a flanking peptide epitope. J Exp Med 1998;188:1017–28.
32. Kuckelkorn U, Ferreira EA, Drung I, Liewer U, Kloetzel PM, Theobald M. The effect of the interferon-gamma-inducible processing machinery on the generation of a naturally tumor-associated human cytotoxic T lymphocyte epitope within a wild-type and mutant p53 sequence context. Eur J Immunol 2002;32: 1368–75.
33. Prang N, Preithner S, Brischwein K, Goster P, Woppel A, Muller J, et al. Cellular and complement-dependent cytotoxicity of Ep-CAM-specific monoclonal antibody MT201 against breast cancer cell lines. Br J Cancer 2005;92:342–9.
34. Zhu X, Belmont HJ, Price-Schiavi S, Liu B, Lee HI, Fernandez M, et al. Visualization of p53(264–272)/HLA-A*0201 complexes naturally presented on tumor cell surface by a multimeric soluble single-chain T cell receptor. J Immunol 2006;176:3223–32.
35. Wittman VP, Woodburn D, Nguyen T, Neethling FA, Wright S, Weidanz JA. Antibody targeting to a class I MHC-peptide epitope promotes tumor cell death. J Immunol 2006;177:4187–95.
36. Sergeeva A, Alatrash G, He H, Ruisaard K, Lu S, Wygant J, et al. An anti-PR1/HLA-A2 T-cell receptor-like antibody mediates complement-dependent cytotoxicity against acute myeloid leukemia progenitor cells. Blood 2011;117:4262–72.
37. McLarty K, Cornelissen B, Cai Z, Scollard DA, Costantini DL, Done SJ, et al. Micro-SPECT/CT with 111In-DTPA-pertuzumab sensitively detects trastuzumab-mediated HER2 downregulation and tumor response in athymic mice bearing MDA-MB-361 human breast cancer xenografts. J Nucl Med 2009;50:1340–8.
38. Overdijk MB, Verploegen S, Ortiz Buijsse A, Vink T, Leusen JH, Bleeker WK, et al. Crosstalk between human IgG isotypes and murine effector cells. J Immunol 2012;189:3430–8.
39. Hong B, van den Heuvel AP, Prabhu VV, Zhang S, El-Deiry WS. Targeting tumor suppressor p53 for cancer therapy: strategies, challenges and opportunities. Curr Drug Targets 2014;15:80–9.
40. Rogel A, Popliker M, Webb CG, Oren M. p53 cellular tumor antigen: analysis of mRNA levels in normal adult tissues, embryos, and tumors. Mol Cell Biol 1985;5:2851–5.
41. Kubbutat MH, Vousden KH. Keeping an old friend under control: regulation of p53 stability. Mol Med Today 1998;4:250–6.

42. Nijman HW, Lambeck A, van der Burg SH, van der Zee AG, Daemen T. Immunologic aspect of ovarian cancer and p53 as tumor antigen. J Transl Med 2005;3:34.
43. Vierboom MP, Nijman HW, Offringa R, van der Voort EI, van Hall T, van den Broek L, et al. Tumor eradication by wild-type p53-specific cytotoxic T lymphocytes. J Exp Med 1997;186:695–704.
44. Zwaveling S, Vierboom MP, Ferreira Mota SC, Hendriks JA, Ooms ME, Sutmuller RP, et al. Antitumor efficacy of wild-type p53-specific CD4(+) T-helper cells. Cancer Res 2002;62:6187–93.
45. Theoret MR, Cohen CJ, Nahvi AV, Ngo LT, Suri KB, Powell DJ Jr., et al. Relationship of p53 overexpression on cancers and recognition by anti-p53 T cell receptor-transduced T cells. Hum Gene Ther 2008; 19:1219–32.
46. Oved K, Ziv O, Jacob-Hirsch J, Noy R, Novak H, Makler O, et al. A novel postpriming regulatory check point of effector/memory T cells dictated through antigen density threshold-dependent anergy. J Immunol 2007;178:2307–17.
47. Michaeli Y, Denkberg G, Sinik K, Lantzy L, Chih-Sheng C, Beauverd C, et al. Expression hierarchy of T cell epitopes from melanoma differentiation antigens: unexpected high level presentation of tyrosinase-HLA-A2 Complexes revealed by peptide-specific, MHC-restricted, TCR-like antibodies. J Immunol 2009;182:6328–41.
48. Van Den Berg HA, Molina-Paris C, Sewell AK. Specific T-cell activation in an unspecific T-cell repertoire. Sci Prog 2011;94:245–64.
49. Adams S, Robbins FM, Chen D, Wagage D, Holbeck SL, Morse HCIII, et al. HLA class I and II genotype of the NCI-60 cell lines. J Transl Med 2005;3:11.
50. Ataie N, Xiang J, Cheng N, Brea EJ, Lu W, Scheinberg DA, et al. Structure of a TCR-mimic antibody with target predicts pharmacogenetics. J Mol Biol 2016;428:194–205.